Olivine

$(Mg,Fe)_2[SiO_4]$

ORTHORHOMBIC (+)(−)

	Forsterite Mg_2SiO_4	Fayalite Fe_2SiO_4
	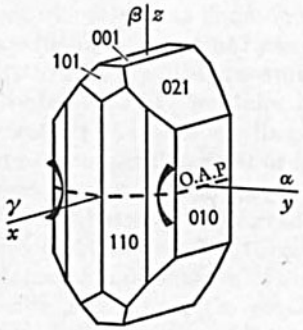	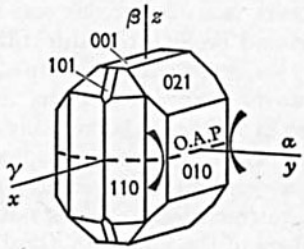
α*	1·635	1·827
β	1·651	1·869
γ	1·670	1·879
δ	0·035	0·052
$2V_\gamma$	82°	134°
	$\alpha=y$, $\beta=z$, $\gamma=x$, O.A.P. (001).	$\alpha=y$, $\beta=z$, $\gamma=x$, O.A.P. (001).
Dispersion:	$r>v$	$r>v$
D†	3·222	4·392
H	7	6½
Cleavage:	{010},{100}imperfect.	{010}moderate, {100}weak.
Twinning:	{100},{011},{012}	{100}
Colour:	Green, lemon-yellow; colourless in thin section.	Greenish yellow, yellow-amber; pale yellow in thin section.
Pleochroism:	—	$\alpha=\gamma$ pale yellow β orange yellow
Unit cell:†	a 4·756 Å b 10·195 Å c 5·981 Å Z=4	a 4·817 Å b 10·477 Å c 6·105 Å Space group *Pbnm*
	Gelatinizes in HCl,	

* Values of refractive indices, birefringence and 2V refer to end-members, between which there is continuous variation.

† Values for synthetic forsterite and fayalite (Yoder & Sahama, 1957).

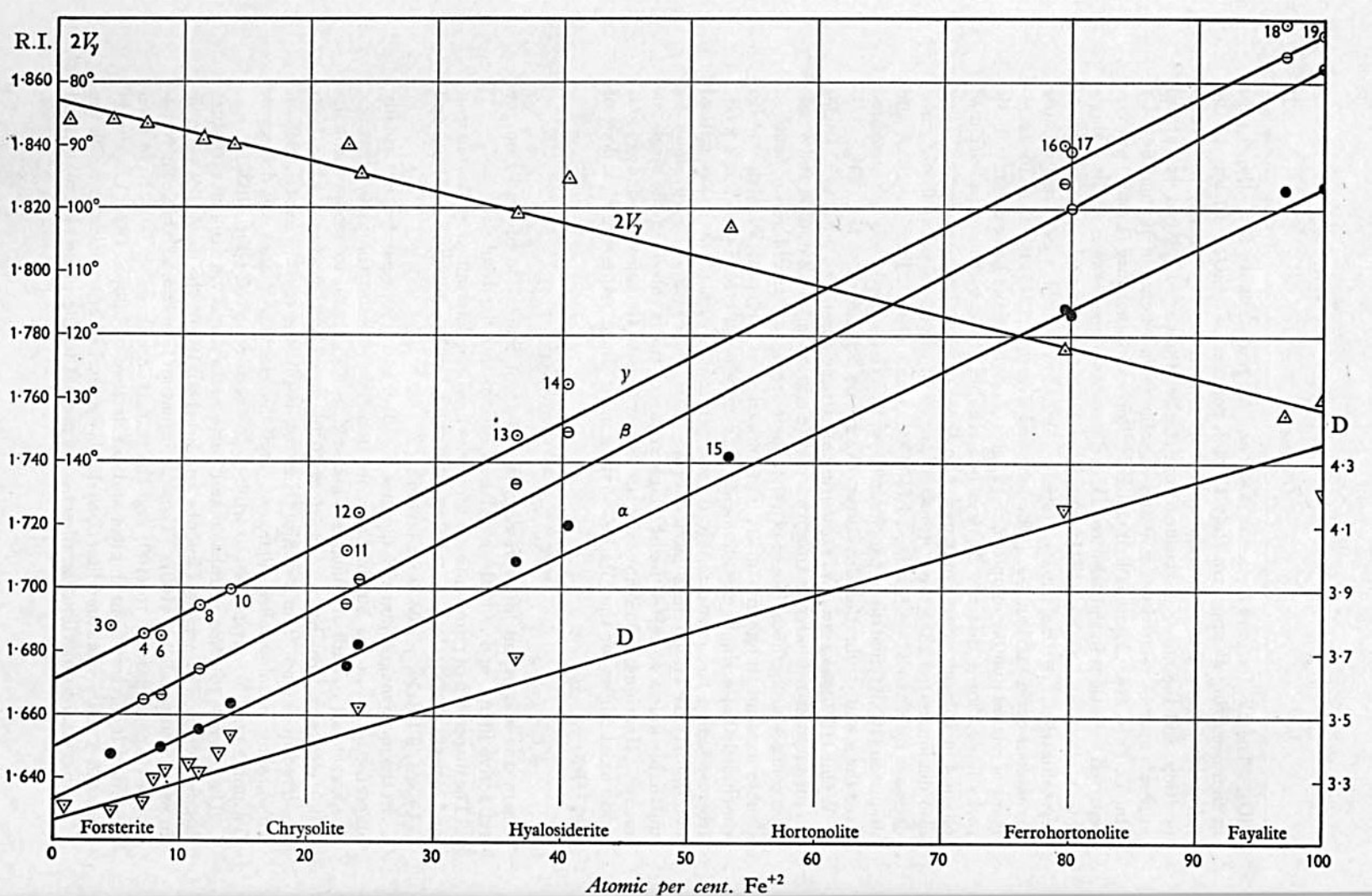
R.I.
$2V_\gamma$
1·860
1·840
1·820
1·800
1·780
1·760
1·740
1·720
1·700
1·680
1·660
1·640
80°
90°
100°
110°
120°
130°
140°
$2V_\gamma$
γ
β
α
D
D
4·3
4·1
3·9
3·7
3·5
3·3
3
4
6
8
10
11
12
13
14
15
16
17
18
19
Forsterite
Chrysolite
Hyalosiderite
Hortonolite
Ferrohortonolite
Fayalite
0
10
20
30
40
50
60
70
80
90
100
Atomic per cent. Fe^{+2}

Diopside
Hedenbergite

$CaMg[Si_2O_6]$
$CaFe^{+2}[Si_2O_6]$

MONOCLINIC (+)

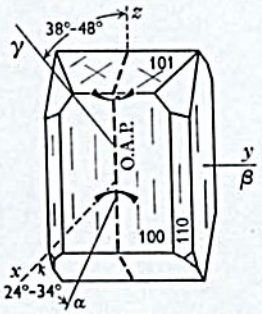

	Diopside†	Hedenbergite†
α	(1·664)‡ 1·664–1·695	1·716–1·726 (1·732)‡
β	(1·6715) 1·672–1·701	1·723–1·730
γ	(1·694) 1·695–1·721	1·741–1·751 (1·757)
δ	(0·030) 0·024–0·031	0·025–0·029 (0·025)
$2V_\gamma$	(59·3°) 50°–60°	52°–62°
$\gamma:z$	(38° 30′) 38°–46°	47°–48°
	$\beta=y$, O.A.P. (010).	$\beta=y$, O.A.P. (010).
Dispersion:	$r>v$, weak to moderate.	$r>v$, strong.
D	3·22–3·38	3·50–3·56
H	$5\frac{1}{2}$–$6\frac{1}{2}$	6

Cleavage: {110} good; {100}, {010} partings. (110): $(1\bar{1}0)\simeq 87°$.

Twinning: {100}, {001}, simple and multiple, common.

Colour:	White, pale green, dark green; diopside colourless in thin section, salite and ferrosalite colourless to pale green.	Brownish green, dark green, black; pale green, yellow green, brownish green in thin section.
Pleochroism:	Diopside non-pleochroic; salite, ferrosalite and hedenbergite may show weak pleochroism:	
	α pale green.	pale green, bluish green.
	β pale greenish brown.	green, light bluish green
	γ pale brownish green.	green, yellow-green.

† Salite and ferrosalite have properties continuous between those of diopside and hedenbergite.

‡ Values for synthetic end-members.

Unit cell :	a Å 9·73	9·85
	b Å 8·91	9·02
	c Å 5·25	5·26
	β 105° 50′	104° 20′

Z = 4. Space group $C2/c$.

Insoluble in HCl.

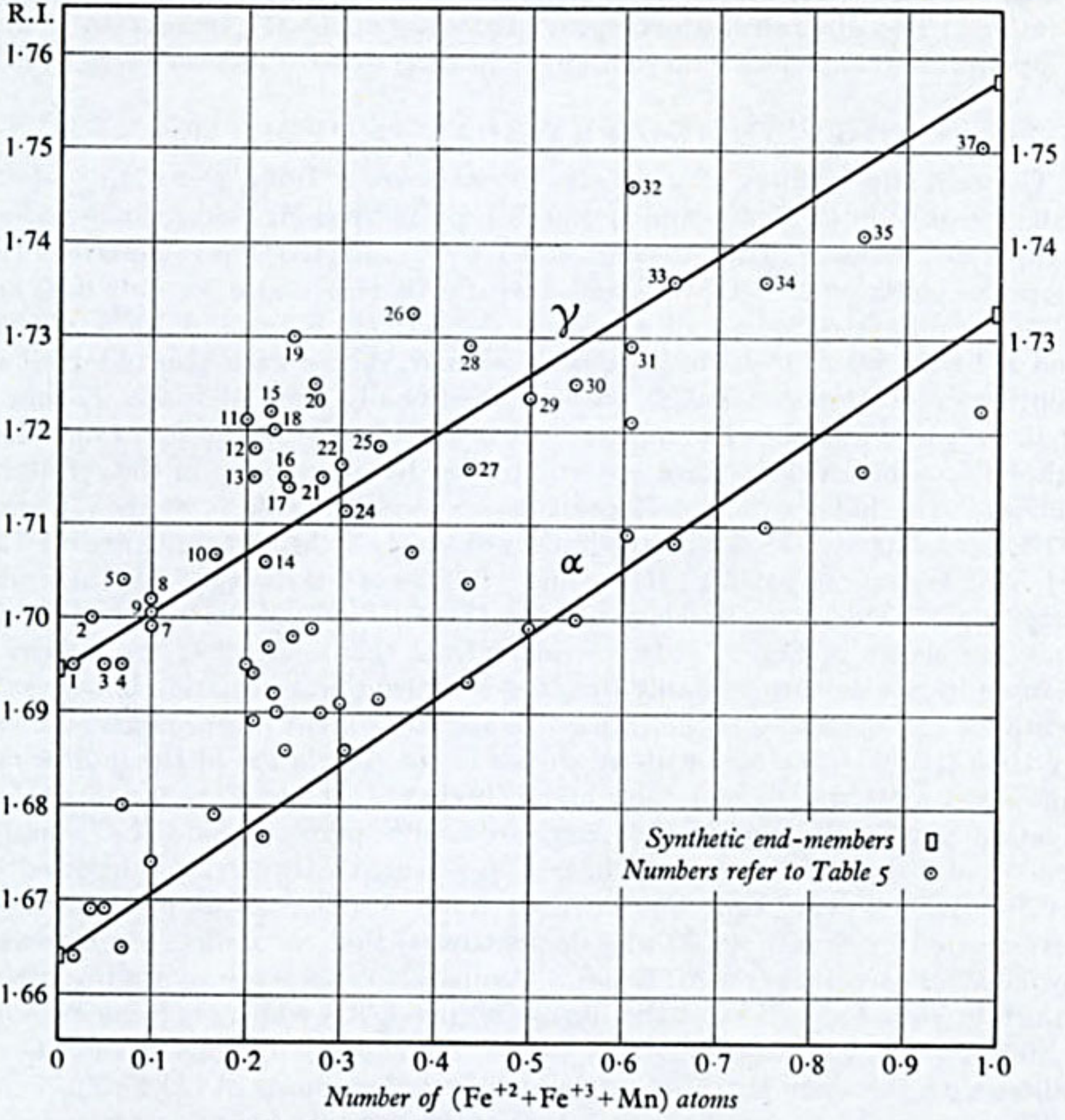
R.I.
1·76
1·75
1·74
1·73
1·72
1·71
1·70
1·69
1·68
1·67
1·66
1·75
1·74
1·73
γ
α
Synthetic end-members
Numbers refer to Table 5
0
0·1
0·2
0·3
0·4
0·5
0·6
0·7
0·8
0·9
1·0
Number of (Fe+2+Fe+3+Mn) atoms

Plagioclase

$Na[AlSi_3O_8]$–$Ca[Al_2Si_2O_8]$

TRICLINIC (+) OR (−)

	High-temperature Albite $NaAlSi_3O_8$	Albite $NaAlSi_3O_8$	Anorthite $CaAl_2Si_2O_8$
α	1·527	1·527	1·577
β	1·532	1·531	1·585
γ	1·534	1·538	1·590
δ	0·007	$0{\cdot}010_5$	$0{\cdot}013_5$
2V	45° (−)	77° (+)	78° (−)

For optic orientation see Fig. 53

Dispersion:	$r<v$	$r<v$	$r<v$
D	2·62	2·63	2·76
H		6–6½	6–6½

Cleavage: {001}Perfect,{010}good.
{110}Poor.

Twinning: (a) Multiple lamellar albite twins [Composition plane (010), twin axis $\perp$ (010)].
(b) Simple Carlsbad twins [Composition plane (010), twin axis z].
(c) Many other normal, parallel and complex twins (see Table 3, p. 22).

Colour: Normally colourless or white, but sometimes yellow, pink, green or black; colourless in thin section.

Unit cell:	a (Å)	8·15	8·14	8·18
	b (Å)	12·88	12·79	12·88
	c (Å)	7·11	7·16	$7{\cdot}08_5\times2$
	α	93° 22′	94° 20′	93° 10′
	β	116° 18′	116° 34′	115° 51′
	γ	90° 17′	87° 39′	91° 13′
Space group[1]:		$C\,\bar{1}$	$C\,\bar{1}$	$P\,\bar{1}$
Z		4	4	4×2

Insoluble in HCl, except anorthite. Soluble in HF or molten Na_2CO_3.

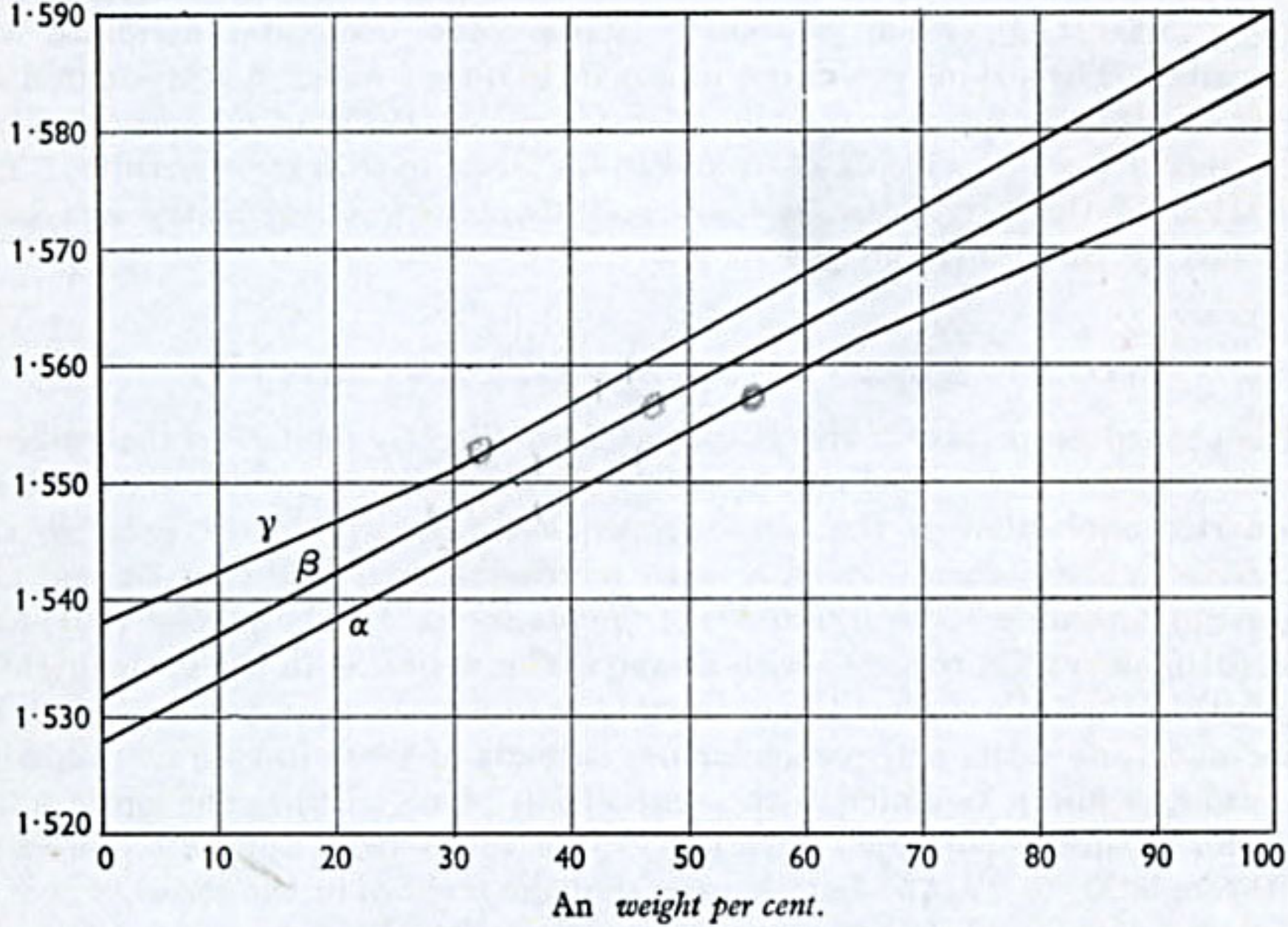

FIG. 48. Determinative chart for the plagioclase series (after Chayes, 1952).

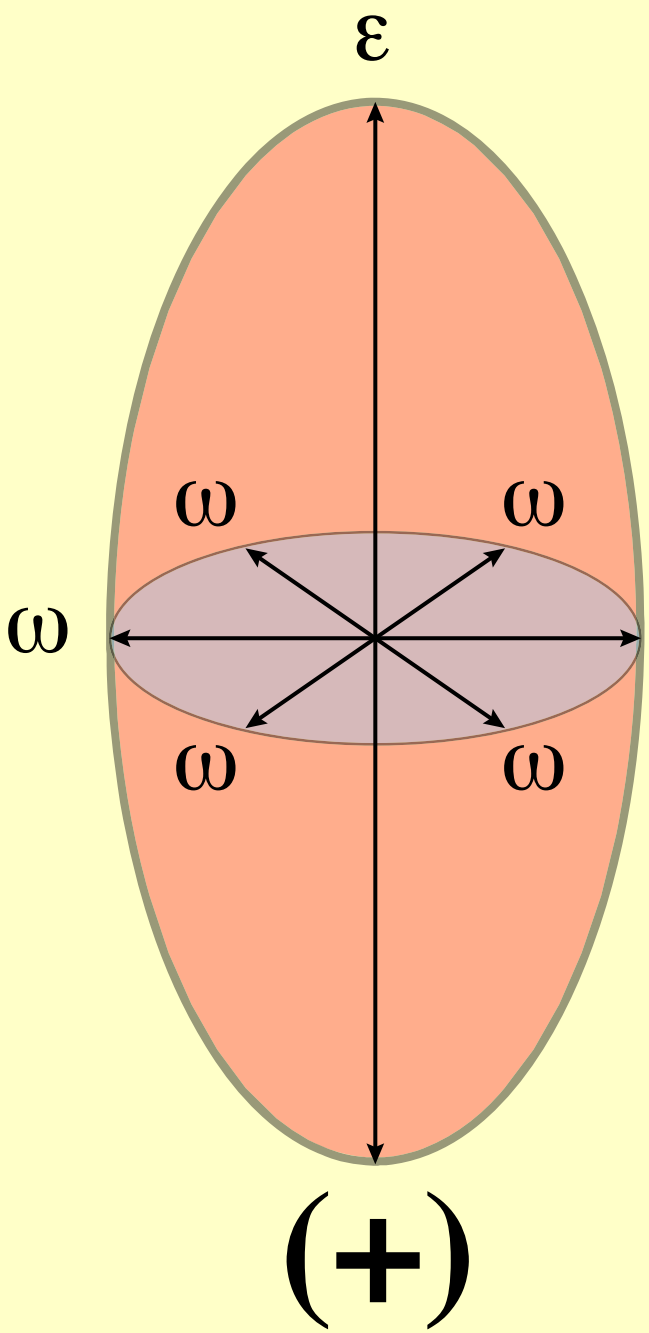
ε
ω
ω
ω
ω
ω

(+)

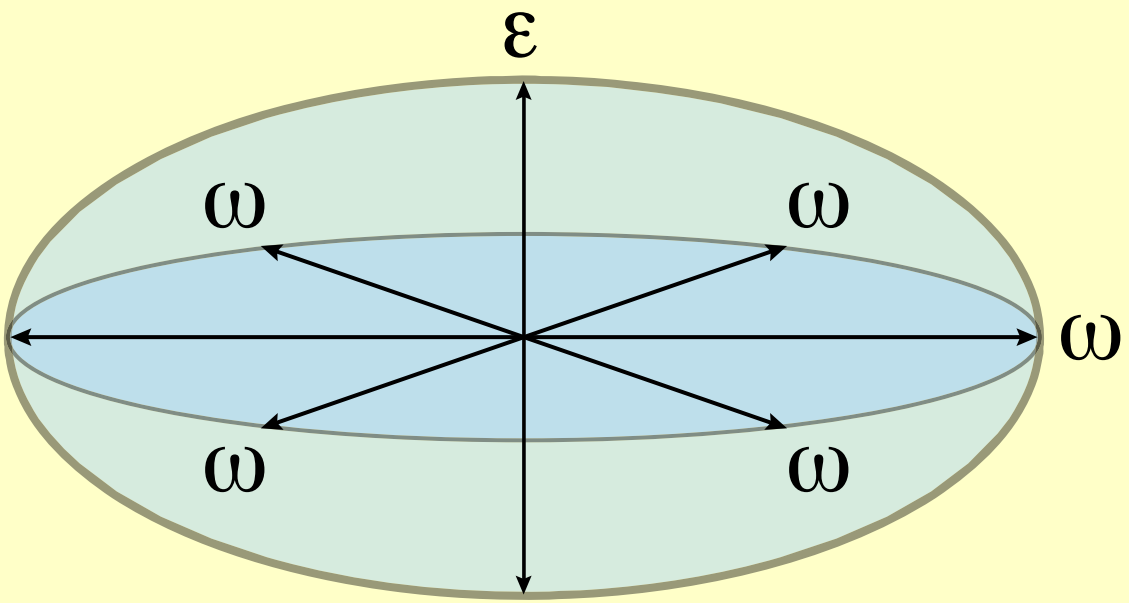
ε
ω
ω
ω
ω
ω

(-)

$$\left(\frac{\mathbf{X}}{\mathbf{n}_\alpha}\right)^2 + \left(\frac{\mathbf{Y}}{\mathbf{n}_\beta}\right)^2 + \left(\frac{\mathbf{Z}}{\mathbf{n}_\gamma}\right)^2 = 1$$

$\mathbf{n}_\alpha$, $\mathbf{n}_\beta$, and $\mathbf{n}_\gamma$ are refrative indices for light vibrating parallel to the X, Y, and Z directions of a Cartesian coordinate system.

Isometric System	$\mathbf{n}_\alpha = \mathbf{n}_\beta = \mathbf{n}_\gamma \equiv \mathbf{n}$				Sphere
Hexagonal System Tetragonal System Trigonal System	$\mathbf{n}_\alpha = \mathbf{n}_\beta \equiv \mathbf{n}_\omega$, $\mathbf{n}_\gamma \equiv \mathbf{n}_\varepsilon$ **c**-axis = $\mathbf{n}_\varepsilon$	$\mathbf{n}_\varepsilon > \mathbf{n}_\omega$ $\mathbf{n}_\varepsilon < \mathbf{n}_\omega$	**(+)** **(–)**	Prolate elipsoid of revolution Oblate elipsoid of revolution	
Orthorhombic System Monoclinic System Triclinic System	$\mathbf{n}_\alpha \le \mathbf{n}_\beta \le \mathbf{n}_\gamma$	$(\mathbf{n}_\gamma - \mathbf{n}_\beta) \ge (\mathbf{n}_\beta - \mathbf{n}_\alpha)$ $(\mathbf{n}_\gamma - \mathbf{n}_\beta) \le (\mathbf{n}_\beta - \mathbf{n}_\alpha)$	**(+)** **(–)**	$\mathbf{2V}_\gamma > \mathbf{2V}_\alpha$ $\mathbf{2V}_\alpha > \mathbf{2V}_\gamma$	General elipsoid General elipsoid

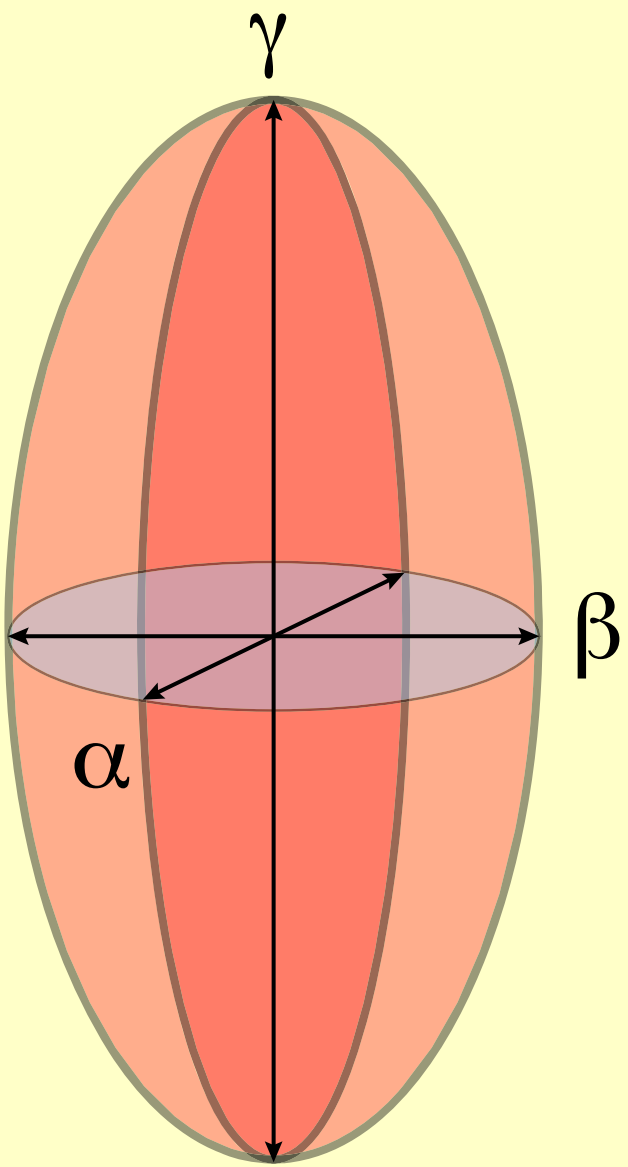

$$\left(\frac{\mathbf{X}}{\mathbf{n}_\alpha}\right)^2 + \left(\frac{\mathbf{Y}}{\mathbf{n}_\beta}\right)^2 + \left(\frac{\mathbf{Z}}{\mathbf{n}_\gamma}\right)^2 = 1$$

$$\gamma > \beta > \alpha$$

$$(+) \quad \gamma - \beta > \beta - \alpha$$

$$(-) \quad \gamma - \beta < \beta - \alpha$$

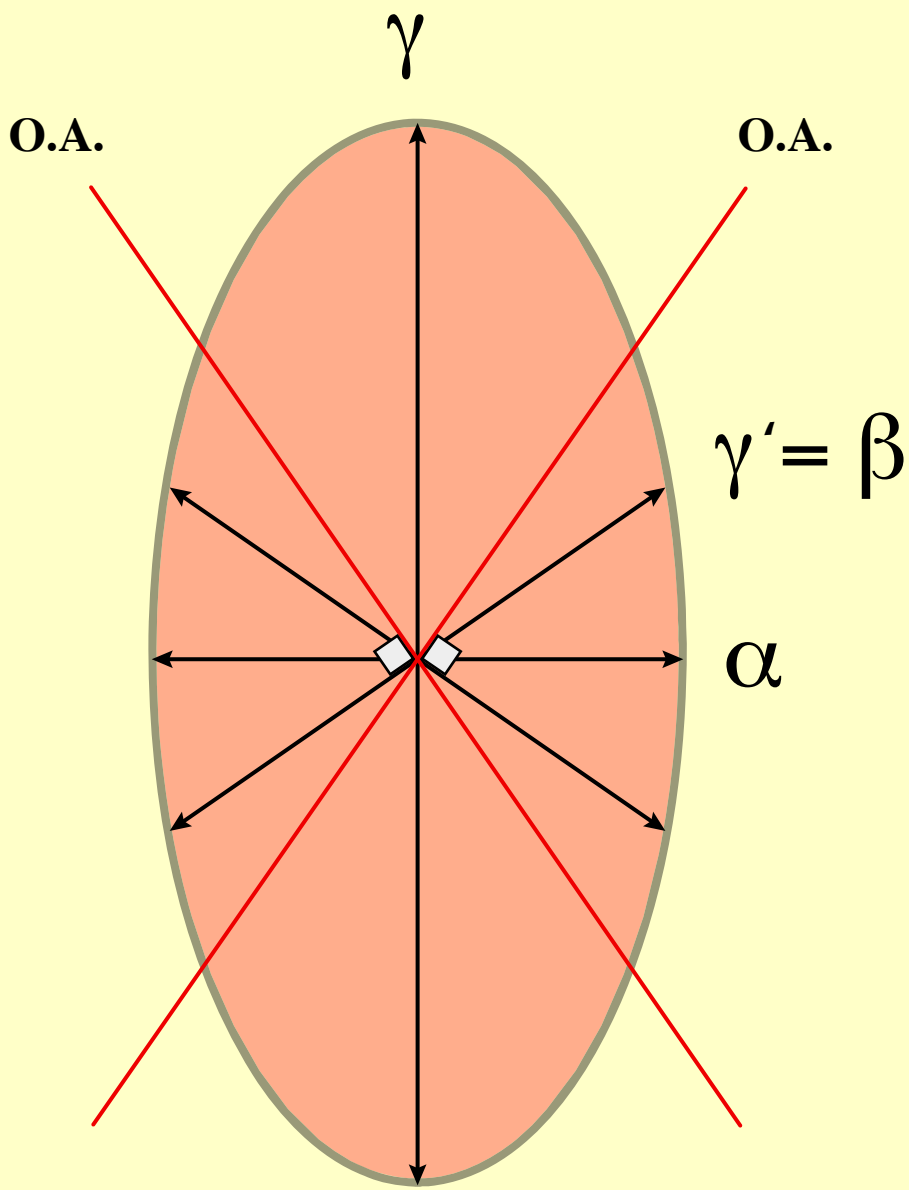
γ
O.A.
O.A.
γ' = β
α

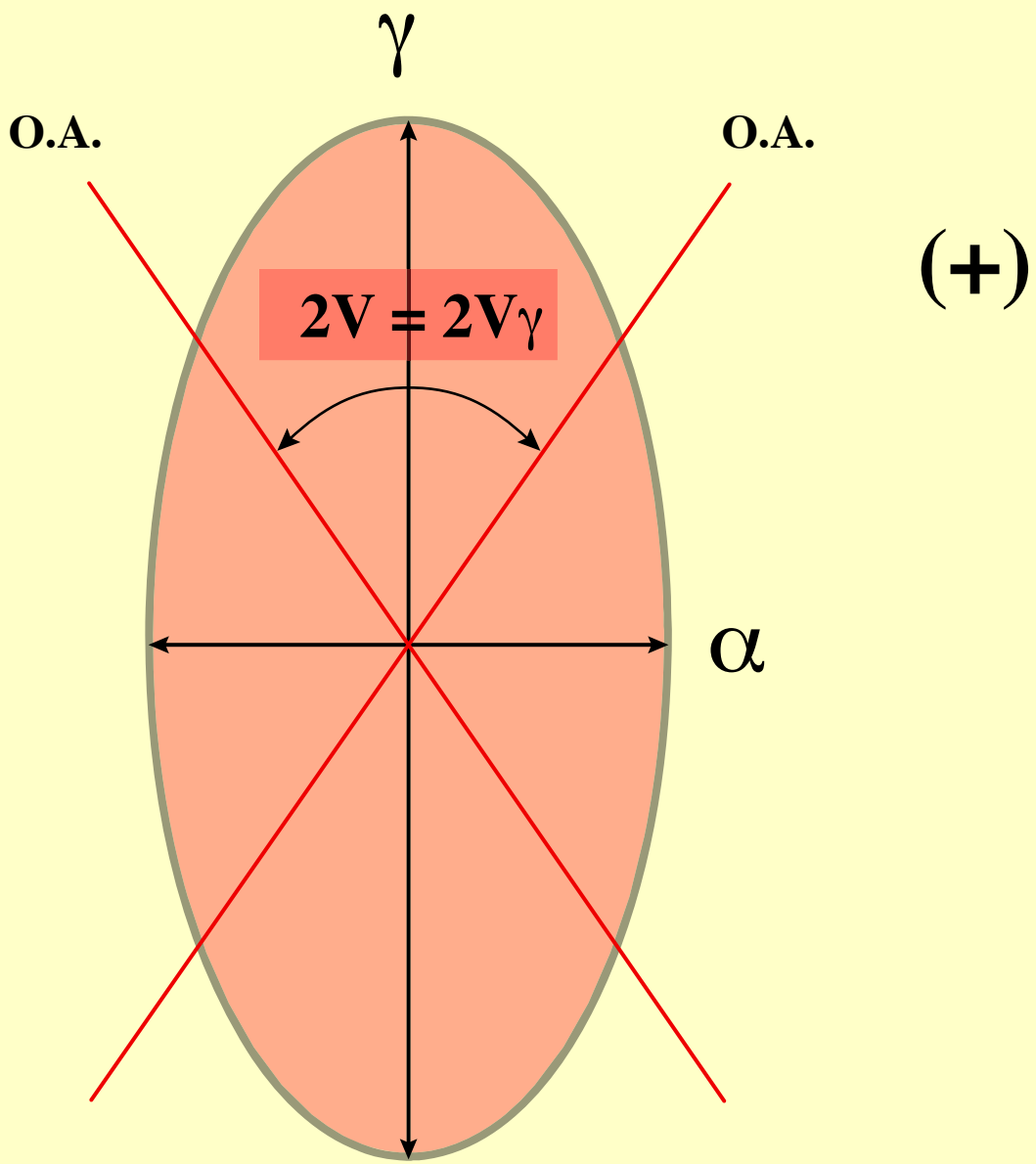
γ
O.A.
O.A.
2V = 2Vγ
α
(+)

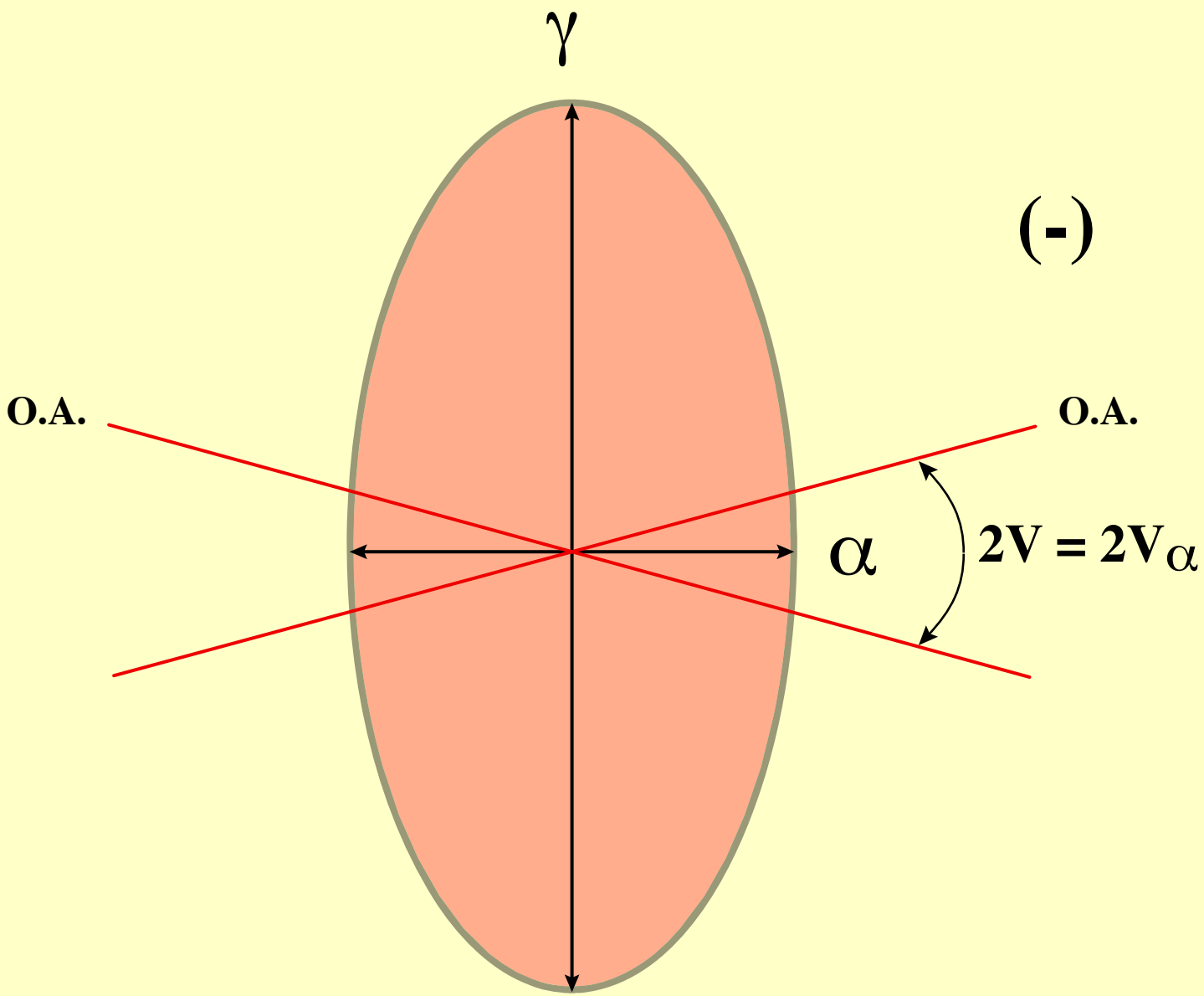
γ
(-)
O.A.
O.A.
α
2V = 2Vα


Upper Cover
Hemicylinder
Battery
Cover
Battery
Compartment
Polarizer
Eye Piece
RI Liquid
Power Switch

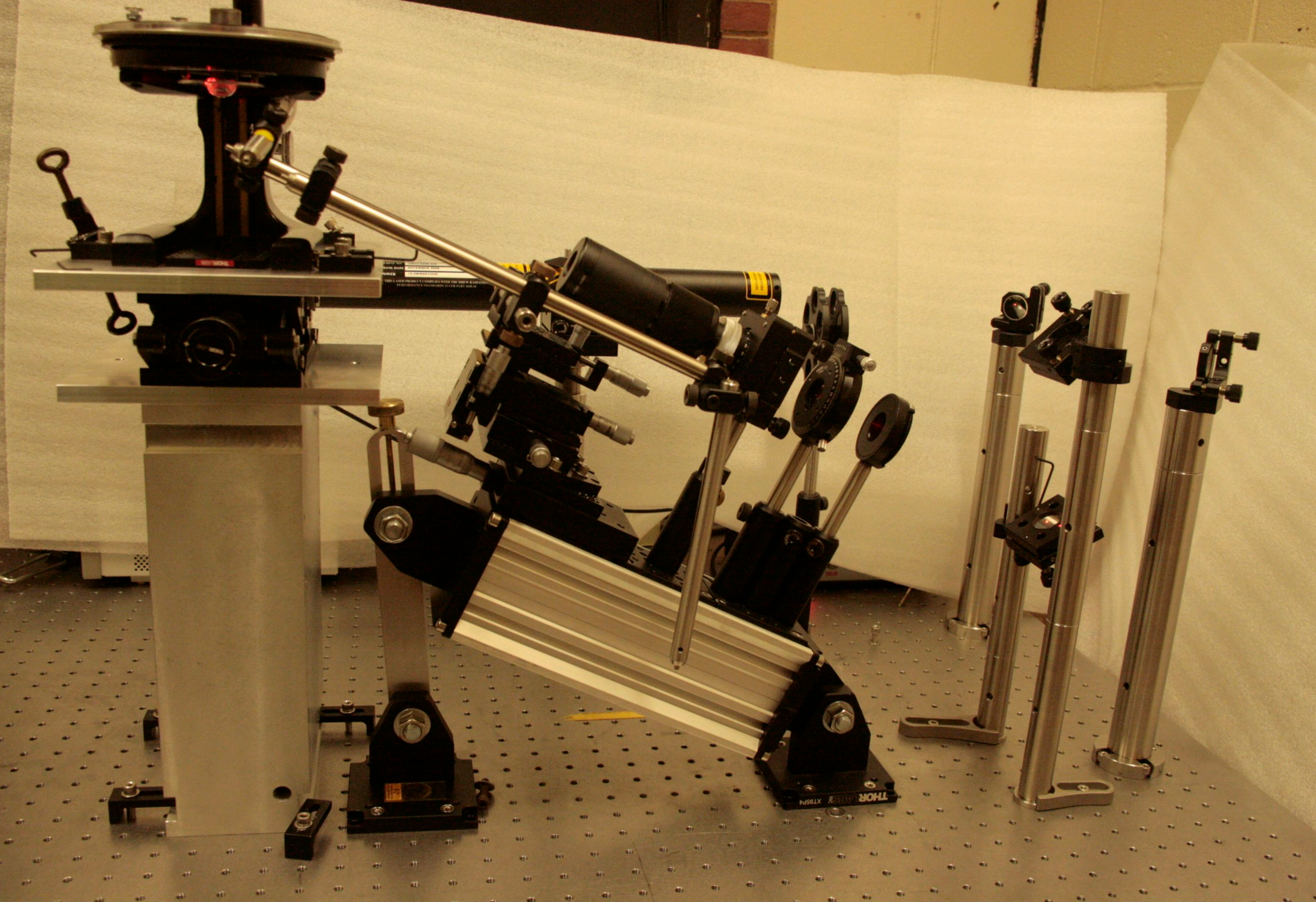
THOR LABS
XT95Pd

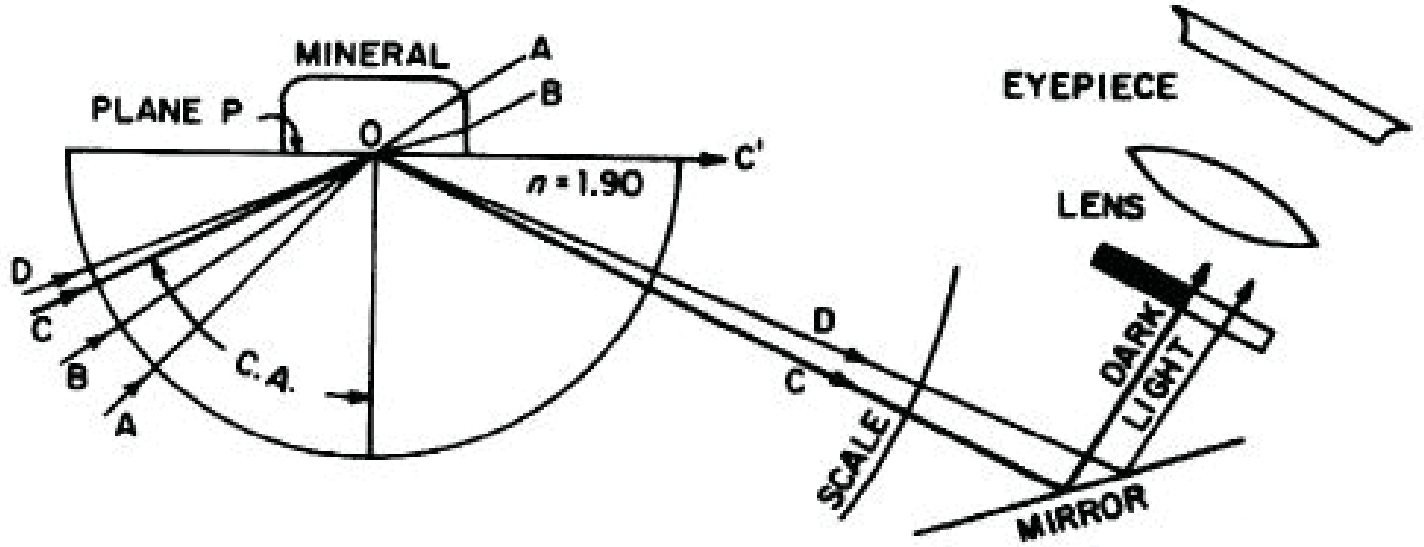

Fig. 1. Longitudinal section through jeweler's refractometer showing light reflected at the critical angle (C.A.) for spinel.

Hurlbut (1984)

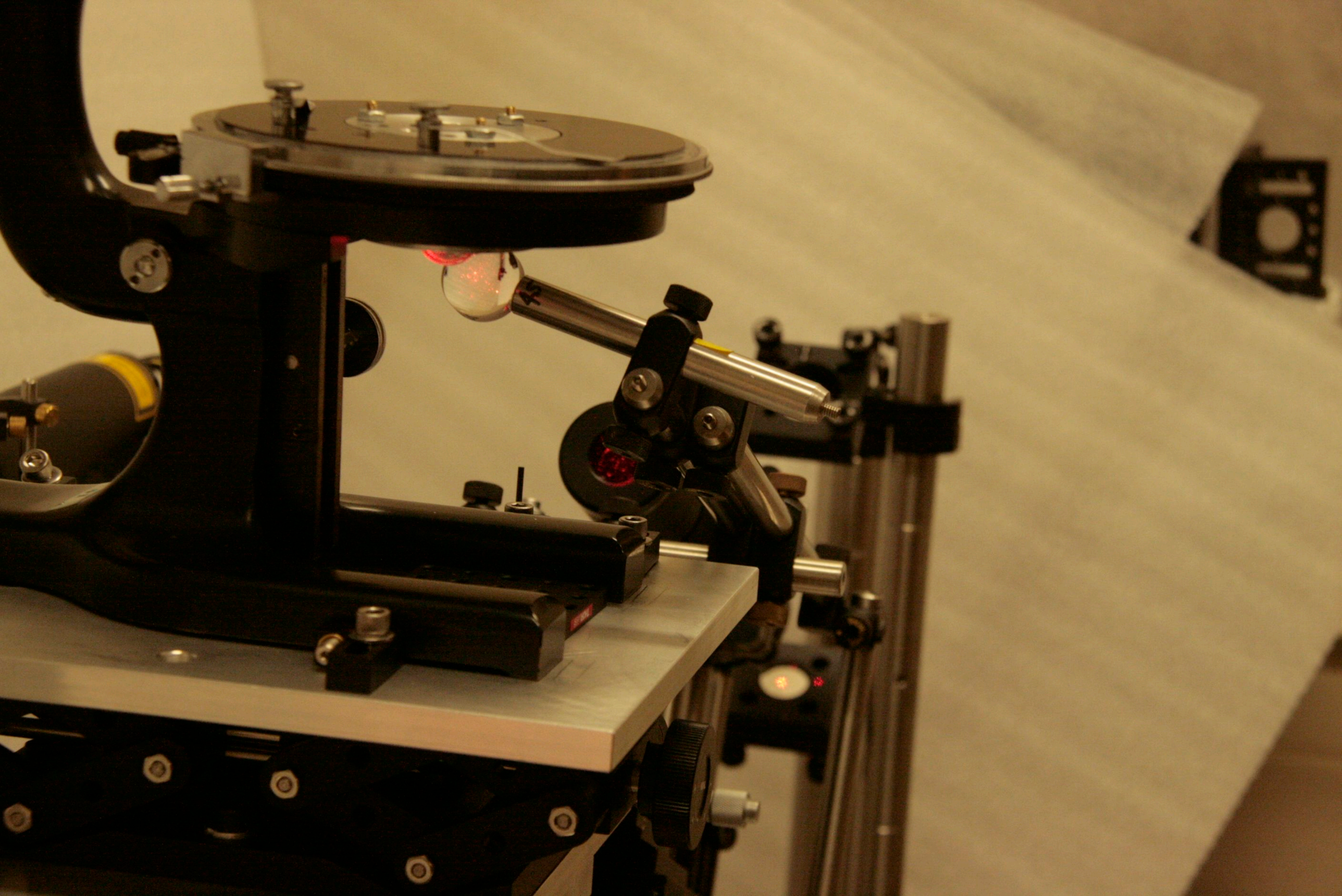

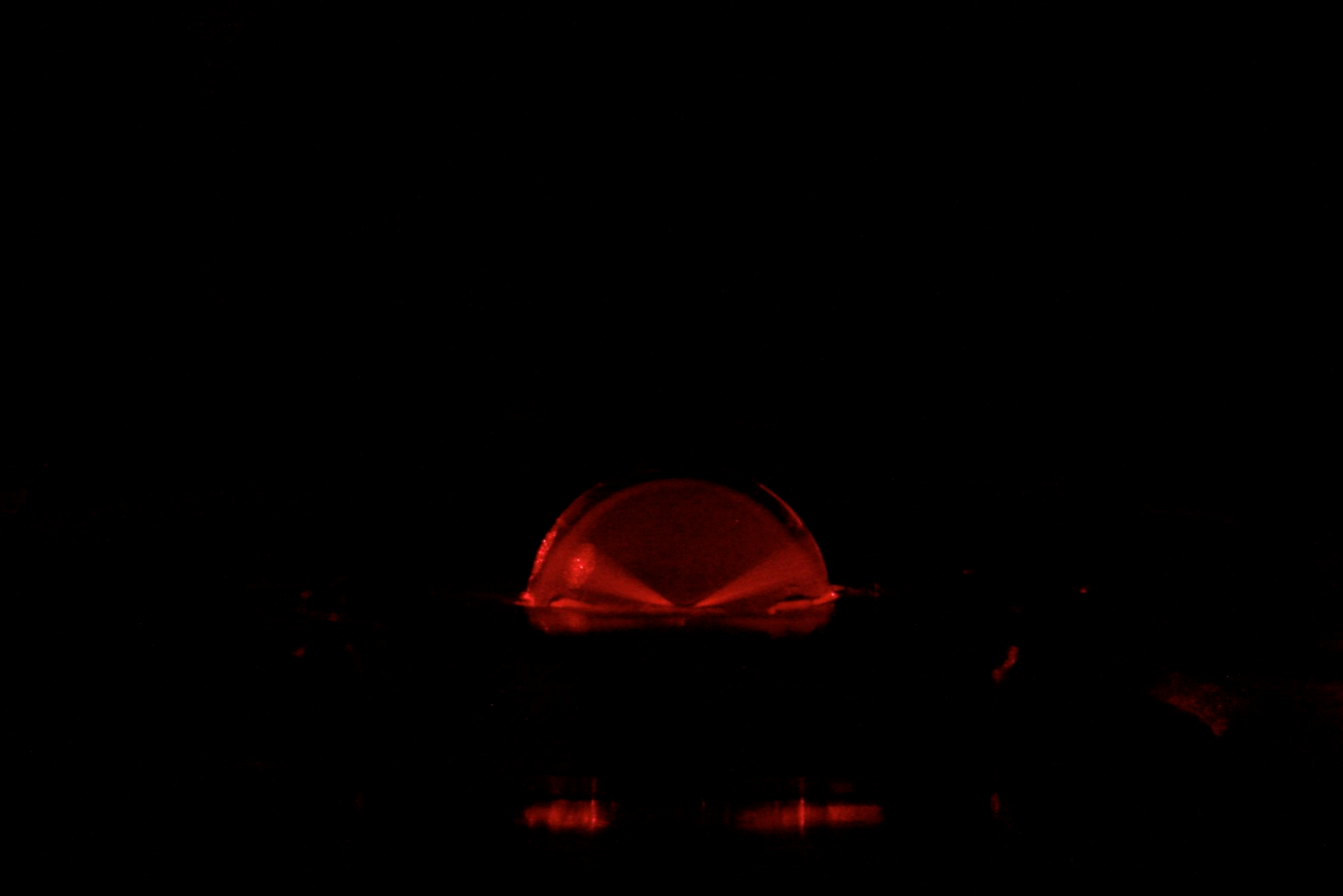

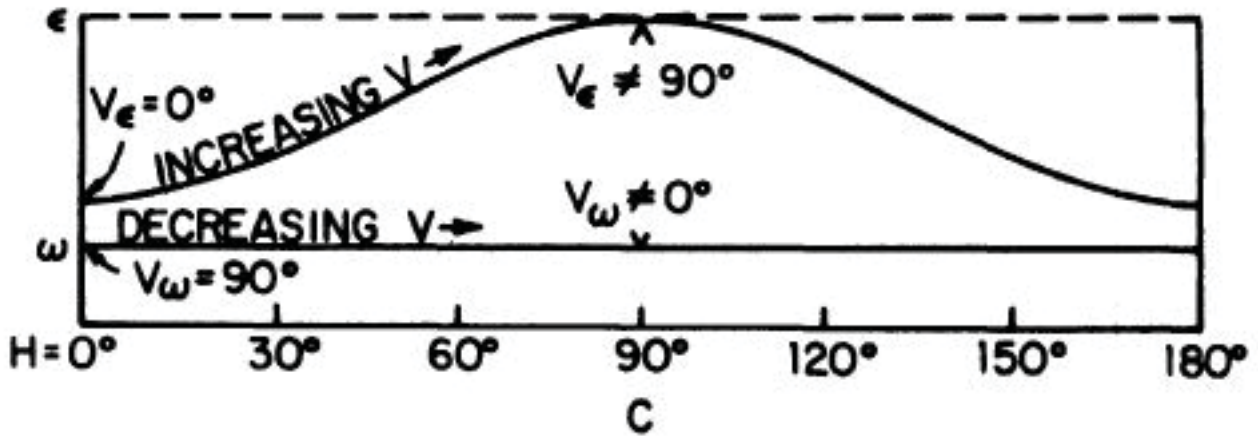

Fig. 4. Variations of refractive index readings of a positive uniaxial crystal as it is rotated on the surface of the refractometer hemicylinder. (A) Optic axis lies in plane P. (B) Optic axis is perpendicular to plane P. (C) Random orientation of plane P.

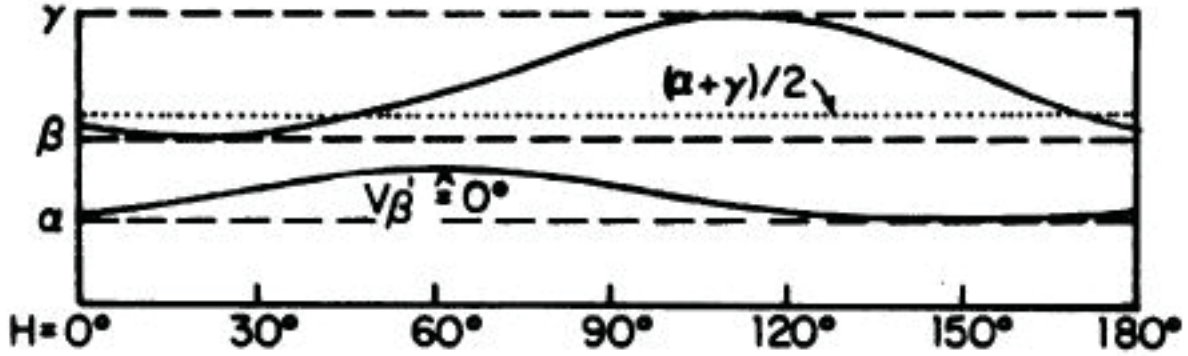

Fig. 10. Variation of refractometer readings with P a random section of a biaxial crystal. Since the minimum reading of the higher index is less than $(\alpha + \gamma)/2$, the crystal is positive.

Hurlbut (1984)